Available on CMS information server

CMS NOTE 2006/047

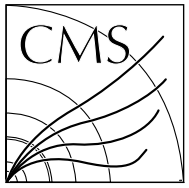

The Compact Muon Solenoid Experiment

CMS Note

Mailing address: CMS CERN, CH-1211 GENEVA 23, Switzerland

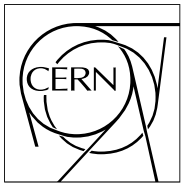

9 January 2006

Standard Model Higgs Discovery Potential of CMS in the $\mathrm{H} \rightarrow \mathrm{WW} \rightarrow \ell\nu\ell\nu$ Channel

G. Davatz, M. Dittmar

Institute for Particle Physics, ETH Zürich, Switzerland

A.-S. Giolo-Nicollerat

CERN, Geneva, Switzerland

Abstract

The discovery potential of the CMS detector for the Standard Model Higgs boson in the $\mathrm{H} \rightarrow \mathrm{WW} \rightarrow \ell\nu\ell\nu$ channel is assessed using a full detector simulation. Sources of systematic uncertainties as well as methods to determine backgrounds from data are discussed. If the Standard Model Higgs boson has a mass between 150 GeV and 180 GeV, it should be observed with a significance of more than 5σ with a luminosity of about 10 fb^{-1}.

1 Introduction

The Higgs boson decay into two W bosons and subsequently into two leptons ($\mathrm{H} \rightarrow \mathrm{WW} \rightarrow \ell\nu\ell\nu$) is expected to be the main discovery channel for the intermediate Higgs-boson mass range, between $2\mathrm{m_W}$ and $2\mathrm{m_Z}$ [1]. The signature of this decay is characterized by two leptons and high missing energy. In this mass range, the $\mathrm{H} \rightarrow \mathrm{WW}$ branching ratio is close to one.

As no narrow mass peak can be reconstructed in this channel, a good background control together with a high signal to background ratio is needed. The most important backgrounds, which give a similar signature as the signal (i.e. two leptons and high missing energy) are continuum WW production and $\mathrm{t\bar{t}}$ production. To reduce these backgrounds, one has to require a small opening angle between the leptons in the plane transverse to the beam and apply a jet veto.

In this note, a study of the CMS discovery potential for this channel is presented. It is based on a full detector simulation. This note concentrates on the Higgs discovery range for Higgs masses between 150 GeV and 180 GeV. The selection cuts are chosen to be mass independent. Three final states are reconstructed: ee, $\mu\mu$ and eμ. In the first part of this note, the signal and background simulation are detailed. Then, the event reconstruction and selection is discussed. Finally, the expected numbers of signal and background events for an integrated luminosity of 1 fb^{-1} are given and a method to normalize each of the background components is proposed.

2 Signal and Background Simulation and Reconstruction

The signal samples were generated using the PYTHIA Monte Carlo generator. The two major Higgs-boson production modes relevant for the mass range under investigation were generated: gluon fusion and vector-boson fusion. Table 1 lists the cross section times $\mathrm{H} \rightarrow \mathrm{WW}$ branching ratio and the sum of branching ratios for W decaying into e, μ and τ[1)] for different Higgs-boson masses. The W boson decay into τ was also simulated but no specific τ reconstruction was applied: τ are selected through their decays into e and μ. The cross sections are shown at leading order (LO), using the PYTHIA predictions, and at next-to-leading order (NLO), using a calculation by M. Spira [2]. In order to get a good NLO estimate for the Higgs-boson production through gluon fusion, the PYTHIA $\mathrm{p_t}$ spectrum was reweighted to the MC@NLO [3] prediction, defining $\mathrm{p_t}$-dependent k-factors as proposed in [4][2)]. The total cross section was then scaled to the NLO cross sections listed in Table 1. Figure 1a) shows the effect of the reweighting on the generated Higgs-boson $\mathrm{p_t}$ spectrum without any cuts applied, for a Higgs-boson mass of 165 GeV. While the effect of introducing the NLO correction changes the cross sections by about factor 2 for the Higgs produced through gluon fusion, it is almost negligible for the Higgs produced through vector-boson fusion.

Table 1: The cross sections times branching ratio ($\mathrm{H} \rightarrow \mathrm{WW}$, $\mathrm{W} \rightarrow \mathrm{e}, \mu, \tau$) for Higgs-boson production through gluon fusion and vector-boson fusion (VBF). The first two columns show the LO results from PYTHIA and the last two show the NLO results [2] used in this study.

	$\sigma^{LO} \times BR(e,\mu,\tau)$ [pb] (PYTHIA)		$\sigma^{NLO} \times BR(e,\mu,\tau)$ [pb]		
	Gluon fusion	VBF	Gluon fusion	VBF	Total
120 GeV	0.26	0.07	0.50	0.06	0.56
130 GeV	0.50	0.13	0.94	0.12	1.06
140 GeV	0.71	0.20	1.39	0.19	1.58
150 GeV	0.89	0.25	1.73	0.25	1.98
160 GeV	1.00	0.31	2.03	0.31	2.34
165 GeV	1.00	0.31	2.04	0.32	2.36
170 GeV	0.97	0.30	1.95	0.31	2.26
180 GeV	0.84	0.27	1.71	0.28	1.99
190 GeV	0.66	0.21	1.29	0.22	1.51
200 GeV	0.56	0.19	1.11	0.19	1.30

For the backgrounds, continuum vector-boson production (WW, ZZ, WZ) was generated using PYTHIA. The $\mathrm{p_t(WW)}$ spectrum was reweighted to the NLO cross section using the same technique as for the signal, as shown

[1)] No particular decay of τ is assumed.

[2)] NNLO cross sections for the Higgs-boson production through gluon fusion were used in reference [4]. The present analysis uses NLO cross sections to be consistent with the other processes which are known at NLO. For Higgs-boson production, the NNLO cross sections are slightly larger than the NLO ones.

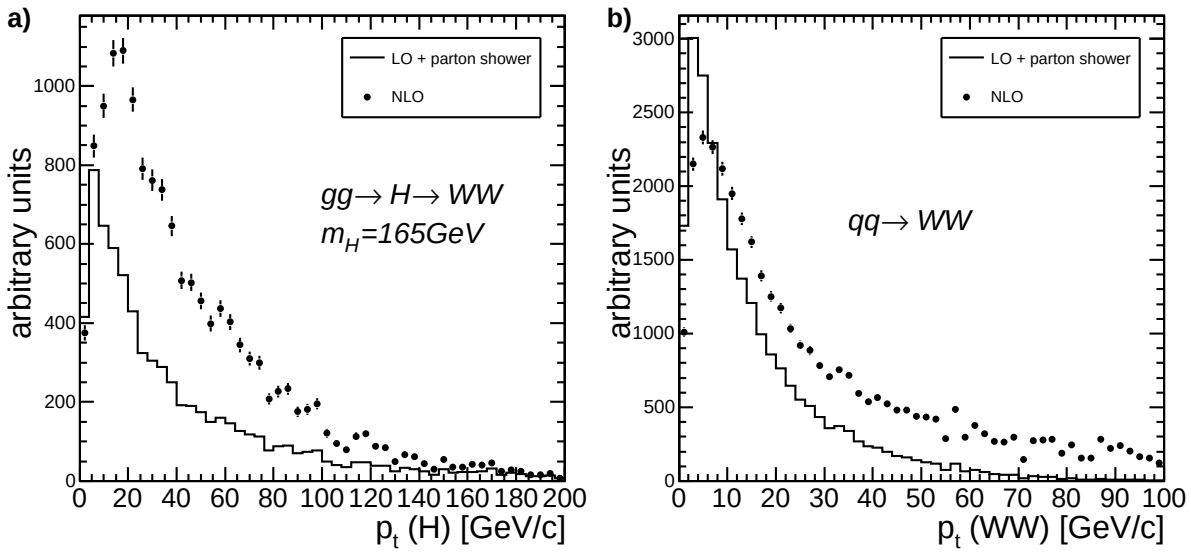

Figure 1: The $\mathrm{p_t}$ spectra produced by PYTHIA (solid line) and after applying $\mathrm{p_t}$-dependent k-factors (dots) for a) A 165 GeV Higgs boson produced through gluon fusion and b) continuum WW production. The statistical uncertainties of the simulated samples are shown. They are the same for LO and NLO.

in Figure 1b). A NLO cross section of respectively 16 pb and 77 pb was assumed for ZZ and WZ production. WW production via gluon fusion was generated using a Monte Carlo provided by N. Kauer [5], with parton shower simulation provided by PYTHIA. Figure 2 shows an example of a Feynman graphs for WW production.

Top production (double resonant, $\mathrm{t\bar{t}}$, and single resonant, tWb) was generated using the TopReX Monte Carlo program [6]. Figure 3 shows two Feynman graphs for the $\mathrm{t\bar{t}}$ and tWb processes. TopReX includes the full spin-correlation structure and an exact treatment of the top mass. The parton shower simulation is provided by PYTHIA. NLO cross sections of respectively 840 pb and 33.4 pb were used for $\mathrm{t\bar{t}}$ and tWb [7]. Table 2 lists the cross sections times branching ratios for the different background processes and compares them with the LO cross section.

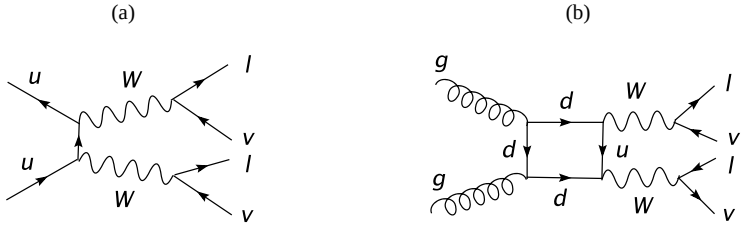

Figure 2: Feynman graphs for a) continuum WW production and b) WW production via gluon fusion.

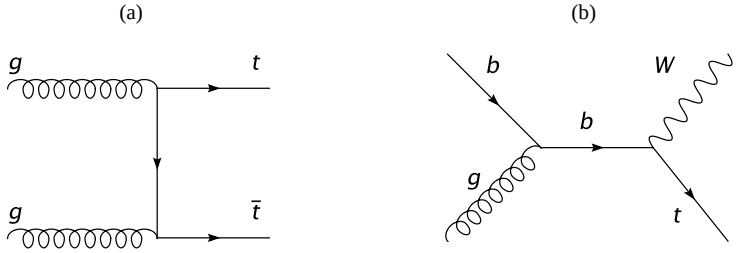

Figure 3: Feynman graphs for a) $\mathrm{t\bar{t}}$ and b) tWb production.

Table 2: The cross sections times branching ratio at LO given by PYTHIA (except for ggWW and tWb) and at NLO for the different background processes [8]. The ggWW cross section is given in reference [5] and is generated using a matrix-element program linked to PYTHIA for the showering. This process is only known at LO. The tWb cross section is from reference [7].

Process	$\sigma^{\mathrm{LO}} \times \mathrm{BR}(\mathrm{e}, \mu, \tau)$ [pb]	$\sigma^{\mathrm{NLO}} \times \mathrm{BR}(\mathrm{e}, \mu, \tau)$ [pb]
$\mathrm{qq} \to \mathrm{WW} \to \ell\nu\ell\nu$	7.4	11.7
$\mathrm{gg} \to \mathrm{WW} \to \ell\nu\ell\nu$	0.48	-
$\mathrm{qq} \to \mathrm{t\bar{t}} \to \mathrm{WbWb} \to \ell\nu\ell\nu\mathrm{bb}$	52.4	86.2
$\mathrm{qq} \to \mathrm{tWb} \to \mathrm{WbWb} \to \ell\nu\ell\nu\mathrm{bb}$	4.9	3.4
$\mathrm{qq} \to \mathrm{ZW} \to \ell\ell\ell\nu$	0.88	1.63
$\mathrm{qq} \to \mathrm{ZZ} \to \ell\ell\ell\ell, \ell\ell\nu\nu, \nu\nu\nu\nu$	1.06	1.52

3 Event Reconstruction

The generated events were passed through a Geant simulation of CMS. Pile-up corresponding to the LHC low luminosity phase was also generated. The events were then reconstructed using the standard CMS software. Table 3 lists the number of signal and background simulated events used in this study together with the Monte Carlo generator version.

Table 3: The number of signal and background simulated events used in this study together with the Monte Carlo generator version.

Channel	Generator version	Number of events
$\mathrm{H} \to \mathrm{WW} \to \ell\ell$ for different m_H	PYTHIA 6.215	20000-50000
$\mathrm{WW} \to \ell\ell$	PYTHIA 6.215	164000
$\mathrm{gg} \to \mathrm{WW} \to \ell\ell$	'ggWW' + PYTHIA 6.227	47000
$\mathrm{t\bar{t}} \to \ell\nu\ell\nu\mathrm{bb}$	TOPREX 4.06	379271
$\mathrm{tWb} \to \ell\nu\ell\nu\mathrm{bb}$	TOPREX 4.06	191000
$\mathrm{WZ} \to \ell\ell\ell\nu$	PYTHIA 6.215	92000
$\mathrm{ZZ} \to \ell\ell/\nu\nu$	PYTHIA 6.215	56000

3.1 Trigger selection

First, the events are required to pass the global Level 1 (L1) trigger. The remaining events have to pass at least one of the following High Level Trigger (HLT) paths: single-electron, double-electron, single-muon or double-muon trigger. The dotted curve in Figure 4a) shows the combined L1+HLT trigger efficiencies as a function of the Higgs-boson mass. The trigger efficiency is reduced since the W boson decays into τ are simulated but no specific τ trigger is used. The dashed curve shows the L1+HLT trigger efficiency for the events where the W bosons decay into electron and muons.

To estimate the numbers of 'useful events' rejected by this trigger requirement it is interesting to look at the trigger efficiency on events having exactly two leptons which fulfill the lepton selection cuts defined in the following section. In Figure 4a) the solid curve shows the trigger efficiency for such events. In this case, the trigger efficiency is higher than 95% on the full mass range. Figure 4b) shows this trigger efficiency for events with muon-muon, electron-muon and electron-electron final states. The trigger efficiency for muons is close to 100% whereas for electrons it is around 96%. This 4% loss could be recovered.

3.2 Lepton selection and reconstruction

Events are required to have exactly two opposite-charge leptons, electrons or muons, with $\mathrm{p_t} > 20$ GeV and $|\eta| < 2$, since the leptons from signal events are mainly central.

The efficiency to reconstruct a muons candidate with $\mathrm{p_t} > 20$ GeV and $|\eta| < 2$ close to a generated muon with $\mathrm{p_t} > 20$ GeV and $|\eta| < 2$ ($\Delta R < 0.15$) is 97%, when looking at events accepted by the HLT. Additional isolation requirements are imposed. The energy in the calorimeters around the muon candidate, within a $\Delta\mathrm{R} = 0.3$ cone, must be lower than 5 GeV and the sum of the $\mathrm{p_t}$ of the tracks within a $\Delta\mathrm{R} = 0.25$ cone around the muon candidate

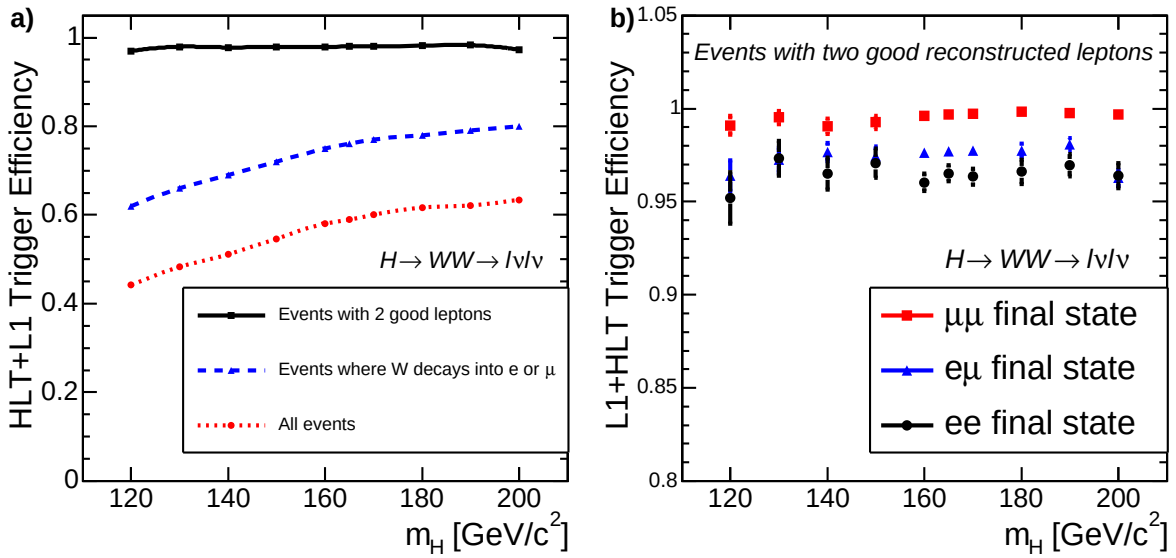

Figure 4: Trigger efficiencies as a function of the Higgs mass. a) L1+HLT trigger efficiency for all generated events (dotted line), events where the W bosons are forced to decay in electrons and muons (dashed line) and on events with exactly two leptons passing the lepton selection cuts (solid line). b) The trigger efficiency for events with two leptons passing the lepton selection cuts for muon-muon (squares), electron-muon (triangles) and electron-electron (circles) final states.

must be lower than 2 GeV. This muon selection has an efficiency of 94% for muons in events which pass the HLT trigger. The separate efficiencies of the selection cuts are listed in Table 4a).

Electrons are reconstructed by combining Super Clusters and tracks. A track is associated to a Super Cluster if their distance satisfies $\Delta R_{track-SC}$ <0.15. Super Clusters are retained only if $E_t(SC) > 20$ GeV and $|\eta(SC)| < 2$. The efficiency to find such a Super Cluster within $\Delta R = 0.2$ of a generated electron with $p_t > 20$ GeV and $|\eta| < 2$ is 92% for events that pass the HLT. An electron candidate must then fulfill the following identification requirements:

- It deposits little energy in the HCAL: $E_{hcal}/E_{ecal} < 0.05$
- There is a precise matching of the electron track and cluster:
  in direction: $|\eta_{track} - \eta_{SC\,corr}| < 0.005$ and $|\phi_{track\,prop} - \phi_{SC}| < 0.02$[3)]
  in magnitude: $E/p > 0.8$ and $|1/E - 1/p| < 0.02$

Finally, the electron candidate must be isolated by requiring $\sum_{tracks} p_t(track)/E_t(SC) < 0.05$ where the sum runs on all the tracks which have:

- $\Delta R_{SC-track} < 0.2$
- $p_t^{track} > 0.9$ GeV
- $|z_{track} - z_{electron}| < 0.2$ cm, where z is the position of the track along the beam line

This electron selection, applied on Super Clusters with an associated track, a transverse energy higher than 20 GeV and a pseudorapidity smaller than 2, has an efficiency of 87%. The efficiencies of each cut are listed in Table 4b).

Finally a cut on the impact parameter significance σ_{IP}, is applied in order to reduce the $b\bar{b}$ background. Each lepton is required to have $\sigma_{IP} < 3$. The two leptons are also required to come from the same vertex by demanding $|z_{lep1} - z_{lep2}| < 0.2$ cm.

The contribution of reducible background processes, like W+jet where one jet is misidentified as a lepton, is expected to be small.

[3)] Where $\eta_{SC\,corr}$ is the Super Cluster pseudorapidity corrected for the vertex position and $\phi_{track\,prop}$ is the track angle propagated in the magnetic field up to the ECAL cluster position.

Table 4: The absolute and, between parentheses, relative efficiency with respect to the previous cut for a)the muon selection-cuts and b) the electron selection-cuts. The cuts are applied on leptons in events that are required to pass the HLT, which accepts mainly good leptons.

(a)

Muon selection	
Cut applied	Selection efficiency
Calorimeter isolation	96%
Tracker isolation	94% (98%)

(b)

Electron selection	
Cut applied	Selection efficiency
Isolation criteria	95%
$E_{hcal}/E_{ecal} < 0.05$	94% (99%)
$\lvert\eta_{track} - \eta_{SC\,corr}\rvert < 0.005$	92% (98%)
$\lvert\phi_{track\,prop} - \phi_{SC}\rvert < 0.02$	91% (99%)
$E/p > 0.8$	91% (100%)
$\lvert 1/E - 1/p\rvert < 0.02$	87% (96%)

3.3 Jet reconstruction

The inclusive cross section for $t\bar{t}$ background is at least 40 times larger than the signal cross section. This background can be strongly reduced by applying a jet veto. The reconstruction of jets is thus fundamental to ensure an efficient background rejection. An important issue is to differentiate between 'real' and 'fake' jets. Fake jets are expected to come from the underlying event, pile-up and noise. Their presence tends to affect signal and background in a similar way.

The jets are reconstructed using a cone algorithm of $\Delta R = 0.5$ on calorimeter towers with $E_t^{tow} > 0.5$ GeV and $E^{tow} > 0.8$ GeV[4]. With the reconstruction software used for this study, the calibration constants are not valid for a jet transverse energy below 25 GeV. However, the real energy of the jets is not needed here, since we only want to apply a jet veto. Thus the raw energy of the jets is used for this study. For the jet energies relevant for our study, $E_t(jet) \approx (1.5 - 2) \cdot E_t(raw)$. In addition the jets are required to be separated from the leptons ($\Delta R_{jet-lepton} > 0.5$) to avoid that electrons and Bremsstrahlung photons are misidentified as jets.

The kinematics of the $t\bar{t}$ process favors central jets, while in the case of the Higgs, relatively more events have high rapidity jets, as shown in Figure 5a) and b). Therefore we apply only a veto on events with central jets. This avoids also potential problems with fake jets in the forward region, as shown in the following.

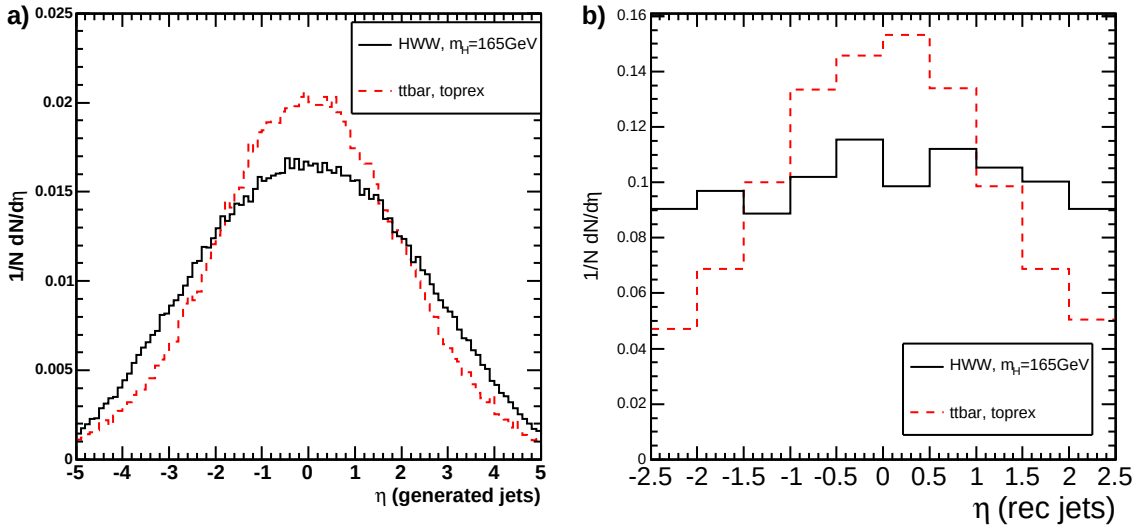

Figure 5: a) The pseudorapidity distribution for the generated jets in the signal sample for $m_H = 165$ GeV (solid line) and the $t\bar{t}$ sample (dashed line) without cuts. b) The same but for the reconstructed jet (built using $E_t^{tow} > 0.5$ GeV and $E^{tow} > 0.8$ GeV, set 2.) with maximum p_t in events with two good reconstructed leptons.

[4] An additional cut on the tower energy is applied in order to reduce the fake jets coming from calorimeter tower noise and which are reconstructed mainly around $|\eta| \approx 0$ if only a cut on the tower transverse energy is applied.

To estimate the contamination due to fake jets, it is useful to look at the generated jets. Here 'generated jets' means jets from the generator tree without detector simulation but using the same algorithms as the reconstructed jets. A jet is then considered 'real' if it can be matched to a generated jet, having $\Delta R_{\mathrm{gen-rec\,jet}} < 0.3$.

Figure 6 shows the fraction of matched jets over the total number of jets as a function of the raw transverse energy of the jet. The dots show the ratio of matched jets over the total number of jets without restricting the jet pseudorapidity and the dots shows the ratio of matched jet over all jets for jets with $|\eta_{\mathrm{jet}}| < 2.5$. The fraction of fake jets decreases when applying a cut on η. For a raw energy above 20 GeV, the number of fake jets is negligible.

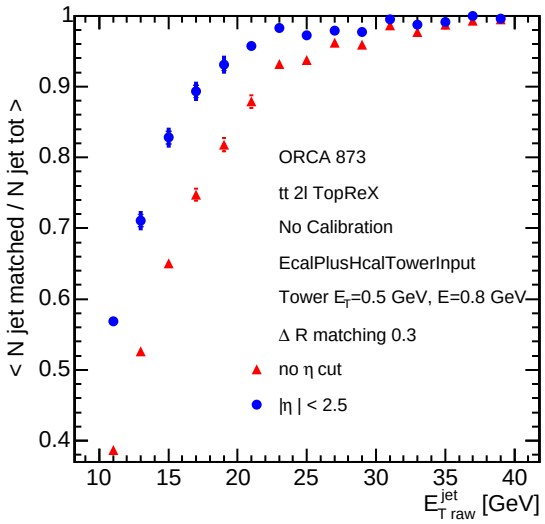

Figure 6: Ratio of reconstructed jets matched to a generated jet over all reconstructed jets as a function of the jet $\mathrm{E_t^{raw}}$. The dots show all jets, while the triangles show all the jets with $|\eta_{\mathrm{jet}}| < 2.5$. For a $\mathrm{E_t^{raw}}$ of 15 GeV for example, this means that around 35% of the reconstructed jets are fake jets, before a cut on $|\eta_{\mathrm{jet}}|$ is applied, and around 18% after the cut is applied.

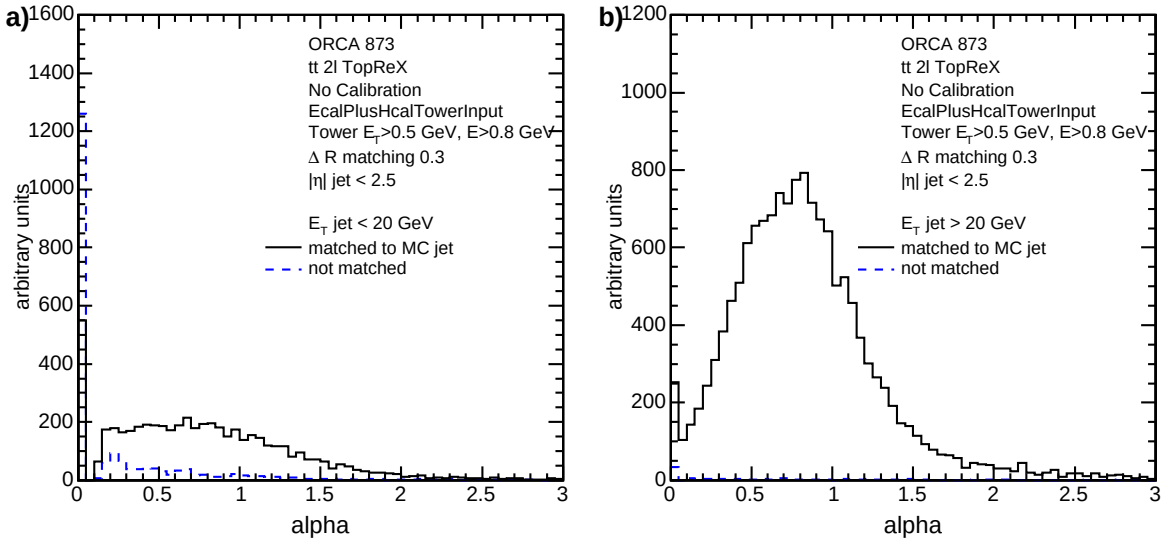

Figure 7: Alpha distribution for a) a jet transverse raw energy smaller than 20 GeV and b) above 20 GeV.

In order to increase the background rejection, jets with a raw transverse energy smaller than 20 GeV should also be vetoed. However, as Figure 6 shows, the number of jets without an associated generated jet, so-called 'fake' jets, is quite high when the raw energies are below 20 GeV. In order to reduce these fake jets, it is useful to consider the track content of the jets, defining the so-called alpha parameter[5]. Alpha is defined to be the ratio of the sum of $\mathrm{p_t}$ of all tracks inside the jet divided by the transverse jet energy in the calorimeter:

[5] This method is based on an idea proposed first by N. Ilina, V. Gavrilov and A. Krokhotin

$$\text{alpha} = \frac{\sum \mathrm{p_t(tracks)}}{\mathrm{E_t(jet)}} \tag{1}$$

For a perfect detector, the alpha parameter of a jet would be on average 0.66, because two thirds of a jet are charged particles. This ratio is smeared and reduced by the detector energy resolution and the fact that particles need a minimal energy in order to be detected. In a fake jet, the alpha parameter looks different, as underlying events contain a lot of low $\mathrm{p_t}$ particles, where the neutral particles leave energy in the ECAL but the charged tracks are curled up in the magnetic field and are then not seen in the tracker. This magnetic field effect leads to an alpha parameter around zero.

To calculate the alpha of a jet, the following tracks are selected: First they have to be 'inside' the jet, i.e. $\Delta \mathrm{R_{track-jet}} < 0.5$. Then they have to come from the event vertex [6], fulfilling $|\mathrm{z_{trk}} - \mathrm{z_{vtx}}|$ <0.4 cm. Finally, these tracks should have more than 5 hits and $\mathrm{p_t} > 2$ GeV.

Figure 7 shows the alpha parameter for $\mathrm{E_t^{raw\,jet}} < 20$ GeV a) and $\mathrm{E_t^{raw\,jet}} > 20$ GeV b). For a jet transverse energy above 20 GeV, almost all jets are matched to the generated jets, as shown in Figure 6. Below 20 GeV however, the unmatched jets tend to have an alpha parameter around 0. Therefore, fake jets can be reduced by requiring alpha > 0.2. Figure 8 shows the fraction of matched jets over the total number of jets as a function of $\mathrm{E_t^{raw}}$ for jets with $|\eta| < 2.5$. The dots show this fraction for jets with alpha > 0.2, whereas the triangles show jets without a cut on alpha. The matching efficiency increases by about 10% for jets between 15 and 20 GeV when the cut on alpha is applied. Adding a cut on alpha for jets with a raw transverse energy between 15 and 20 GeV allows to efficiently veto jets, keeping the fake rate low and a reasonable efficiency for the signal. This jet veto corresponds roughly to requiring that no quark or gluon with energy 40 GeV or above is produced[7].

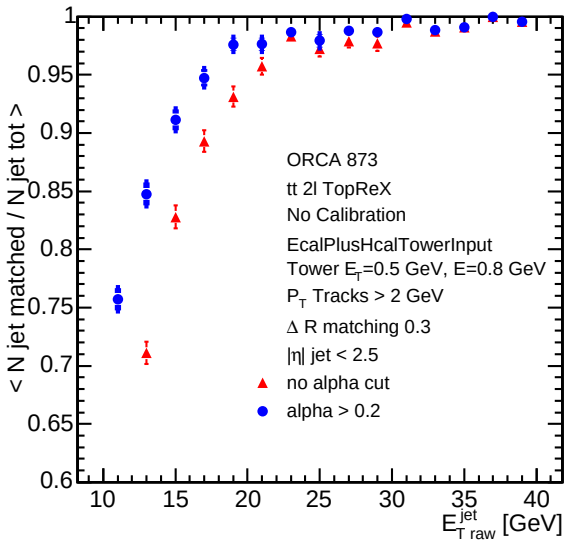

Figure 8: Fraction of matched jets to a generated jet over all reconstructed jets as a function of $\mathrm{E_{T\,raw}^{jet}}$ for jets built with a constant tower energy cut and requiring $|\eta_{\mathrm{jet}}| < 2.5$, shown for jets reconstruction from set 2. The dots are the ones where a cut on alpha is applied, whereas on the crosses no cut on alpha is applied.

In summary, for this study, jets are reconstructed using a cone algorithm with a cone size 0.5, using calorimeter towers with raw energy of $\mathrm{E_t^{tow}} > 0.5$ GeV and $\mathrm{E^{tow}} > 0.8$ GeV. Currently no calibration is applied on the jet energy. In order to reduce fake jets, we require that jets have $|\eta| < 2.5$. and for jets with $\mathrm{E_t^{raw}}$ between 15 and 20 GeV, it is further required that the sum of transverse momenta of all tracks associated to the jet represents a substantial fraction of the transverse jet energy (alpha > 0.2). For the signal selection, the events containing such jets will be vetoed.

[6] The event vertex is defined as the mean z position of the two leptons.

[7] Alternative methods were studied to implement the jet veto. For example, since the jets from $\mathrm{t\bar{t}}$ are b-jets, a possibility would be to veto jets that have tracks with an impact parameter significance higher than 2.

3.4 Missing energy reconstruction

The missing energy is reconstructed by summing up the raw energy of all ECAL and HCAL towers, and correcting for muons. Since a jet veto is applied in the signal selection, further corrections to the missing energy did not lead to a significant improvement.

4 Kinematic Selection and Results

Starting with two oppositely-charged leptons fulfilling the cuts described above, these additional selection cuts were applied:

- $\mathrm{E_t^{miss}}$ >50 GeV (missing transverse energy)
- $\phi_{\ell\ell} < 45^\circ$ (angle between the leptons in the transverse plane)
- 12 GeV $< \mathrm{m}_{\ell\ell} <$ 40 GeV (invariant mass of the two leptons)
- No jet with $\mathrm{E_t^{raw}} > 15$ GeV and $|\eta|$ <2.5 (jet veto)
- 30 GeV $< \mathrm{p_t^{\ell\,max}} <$ 55 GeV (lepton with the maximal $\mathrm{p_t}$)
- $\mathrm{p_t^{\ell\,min}} >$ 25 GeV (lepton with the minimal $\mathrm{p_t}$)

These cuts were optimized to discover a Higgs boson with a mass between 160 and 170 GeV [8]. Each cut value was varied and the value which maximized the signal significance and signal to background ratio was retained. Tables 5, 6 and 7 summarize, for the Higgs-boson signal at different masses and the backgrounds, the number of expected events after each selection cut for 1 fb^{-1} integrated luminosity. The relative efficiencies are given in parentheses. The last line shows the total selection efficiency together with the error coming from the limited Monte Carlo statistics.

Table 5: The expected number of events for an integrated luminosity of 1 fb^{-1} for the signal with Higgs masses between 120 and 160 GeV. The relative efficiency with respect to the previous cut is given in parentheses. The last line shows the total selection efficiency together with the uncertainty from the limited Monte Carlo statistics.

	$\mathrm{H\to WW}$ $\mathrm{m_H = 120GeV}$	$\mathrm{H\to WW}$ $\mathrm{m_H = 130GeV}$	$\mathrm{H\to WW}$ $\mathrm{m_H = 140GeV}$	$\mathrm{H\to WW}$ $\mathrm{m_H = 150GeV}$	$\mathrm{H\to WW}$ $\mathrm{m_H = 160GeV}$
$\sigma \times \mathrm{BR}(\mathrm{e},\mu,\tau)$ [fb]	560	1060	1570	1970	2330
L1+HLT	247 (44%)	511 (48%)	802 (51%)	1077 (55%)	1353 (58%)
2 lep, $\|\eta\| < 2$, $\mathrm{p_t} > 20$GeV $\sigma_{\mathrm{IP}} > 3$, $\|\Delta \mathrm{z_{lep}}\| < 0.2$ cm	30 (12%)	88 (17%)	171 (21%)	264 (25%)	359 (27%)
$\mathrm{E_t^{miss}} > 50$ GeV	12 (39%)	37 (42%)	88 (52%)	150 (57%)	240 (67%)
$\phi_{\ell\ell} < 45$	6.6 (55%)	20 (53%)	44 (50%)	76 (51%)	139 (58%)
12 GeV $< \mathrm{m}_{\ell\ell} <$ 40 GeV	5.5 (83%)	15 (76%)	34 (76%)	56 (73%)	107 (77%)
Jet veto	2.3 (41%)	7.4 (50%)	17 (49%)	29 (52%)	56 (52%)
30 GeV$< \mathrm{p_t^{\ell\,max}} <$55 GeV	1.6 (72%)	5.0 (68%)	13 (77%)	23 (80%)	49 (89%)
$\mathrm{p_t^{\ell\,min}} >$25 GeV	0.80 (49%)	3.2 (63%)	8.2 (64%)	17 (75%)	42 (85%)
$\varepsilon_{\mathrm{tot}}$	$(0.14 \pm 0.03)\%$	$(0.30 \pm 0.04)\%$	$(0.52 \pm 0.05)\%$	$(0.86 \pm 0.07)\%$	$(1.80 \pm 0.06)\%$

The cut on $\mathrm{E_t^{miss}}$ reduces the contribution from Drell-Yan ($\mathrm{pp} \to \gamma, \mathrm{Z}$) events, which has a sharp peak around 15 GeV. It also reduces the WW contribution since the missing energy for this process peaks around 30 GeV, compared to 65 GeV for a 165 GeV Higgs boson, as shown in Figure 9a).

The cuts on $\phi_{\ell\ell}$ and $\mathrm{m}_{\ell\ell}$ reduce particularly WW continuum production. The cut $\mathrm{m}_{\ell\ell} < 40$ GeV reduces Drell-Yan events but also WW and $\mathrm{t\bar{t}}$ events which have a longer $\mathrm{m}_{\ell\ell}$ tail than the signal (Figure 9b)). The cut $\mathrm{m}_{\ell\ell} < 12$ GeV removes potential background from b-resonances. It has a 97% efficiency on a 165 GeV Higgs-boson signal.

The jet veto is mostly efficient against the $\mathrm{t\bar{t}}$ background. A jet veto applied on the jet raw transverse energy at 15 GeV corresponds roughly to a veto on the corrected transverse energy of 25 GeV. For the ggWW background a jet veto is applied. However an efficiency of 1 is conservatively assumed for this cut, since this process is only known at LO [14]. Another possibility for further investigation would be to use the same k-factors as for the signal, since it is also produced with two gluons in the initial state.

Table 6: The expected number of events for an integrated luminosity of 1 fb^{-1} for Higgs-boson masses between 165 and 200 GeV. The relative efficiency with respect to the previous cut is given in parentheses. The last line shows the total selection efficiency together with the uncertainty from the limited Monte Carlo statistics.

	$H \to WW$ $m_H = 165GeV$	$H \to WW$ $m_H = 170GeV$	$H \to WW$ $m_H = 180GeV$	$H \to WW$ $m_H = 190GeV$	$H \to WW$ $m_H = 200GeV$
$\sigma \times BR(e, \mu, \tau)$ [fb]	2360	2250	1980	1500	1300
L1+HLT	1390 (59%)	1350 (60%)	1220 (62%)	933 (62%)	824 (63%)
2 lep, $\lvert\eta\rvert < 2$, $p_t > 20$GeV $\sigma_{IP} > 3$, $\lvert\Delta z_{lep}\rvert < 0.2$ cm	393 (28%)	376 (28%)	346 (28%)	268 (29%)	270 (33%)
$E_t^{miss} > 50$ GeV	274 (70%)	263 (70%)	239 (69%)	184 (69%)	181 (67%)
$\phi_{\ell\ell} < 45$	158 (58%)	139 (53%)	110 (46%)	70 (38%)	58 (32%)
12 GeV $< m_{\ell\ell} <$ 40 GeV	119 (75%)	100 (72%)	71 (64%)	37 (53%)	27 (46%)
Jet veto	63 (53%)	51 (51%)	35 (50%)	19 (52%)	12 (46%)
30 GeV$< p_t^{\ell\,max} <$55 GeV	53 (85%)	41 (82%)	24 (68%)	13 (68%)	8.7 (69%)
$p_t^{\ell\,min} >$25 GeV	46 (86%)	33 (80%)	18 (76%)	9.2 (71%)	6.1 (71%)
ε_{tot}	$(1.95 \pm 0.06)\%$	$(1.47 \pm 0.05)\%$	$(0.91 \pm 0.07)\%$	$(0.61 \pm 0.06)\%$	$(0.47 \pm 0.05)\%$

Table 7: The expected number of events for an integrated luminosity of 1 fb^{-1} for the backgrounds. The relative efficiency with respect to the previous cut is given in parentheses. The last line shows the total selection efficiency together with the uncertainty from the limited Monte Carlo statistics.
[1] Note: For ggWW a jet veto is applied but its efficiency is conservatively scaled to 1 as this process is only known at LO [14].

	$qq \to WW$	$gg \to WW$	$t\bar{t}$	tWb	WZ	ZZ
$\sigma \times BR(e, \mu, \tau)$ [fb]	11700	480	86200	3400	1630	1520
L1+HLT	6040 (52%)	286 (60%)	57380 (67%)	2320 (68%)	1062 (65%)	485 (32%)
2 lep, $\lvert\eta\rvert < 2$, $p_t > 20$GeV $\sigma_{IP} > 3$, $\lvert\Delta z_{lep}\rvert < 0.2$ cm	1398 (23%)	73 (26%)	15700 (27%)	676 (29%)	247 (23%)	163 (34%)
$E_t^{miss} > 50$ GeV	646 (46%)	43 (59%)	9332 (59%)	391 (58%)	103 (42%)	70 (43%)
$\phi_{\ell\ell} < 45$	59 (9.2%)	11 (26%)	1649 (18%)	65 (17%)	14 (13%)	10 (15%)
12 GeV $< m_{\ell\ell} <$ 40 GeV	29 (49%)	6.5 (57%)	661 (40%)	28 (43%)	1.8 (13%)	1.3 (12%)
Jet veto	23 (80%)	6.5[1]	24 (3.6%)	3.6 (13%)	1.2 (70%)	0.98 (75%)
30 GeV$< p_t^{\ell\,max} <$55 GeV	17 (74%)	5.1 (78%)	13 (54%)	2.3 (63%)	0.85 (70%)	0.46 (47%)
$p_t^{\ell\,min} >$25 GeV	12 (69%)	3.7 (73%)	9.8 (74%)	1.4 (62%)	0.50 (58%)	0.35 (76%)
ε_{tot}	$(0.103\pm$ 0.008)%	$(0.77\pm$ 0.04)%	$(0.011\pm$ 0.002)%	$(0.041\pm$ 0.005)%	$(0.031\pm$ 0.006)%	$(0.023\pm$ 0.006)%

Figure 9c) shows the $\phi_{\ell\ell}$ distribution for the signal and the different backgrounds after all cuts are applied. A clear signal is seen. Figures 11 and 12 and Table 8 show the signal to background ratio, the signal significance with 5 fb^{-1} and the luminosity needed for a 5σ discovery for different Higgs masses. The signal significance is defined as the probability that the observed background, N_B, fluctuates above the sum of the signal and background, $N_S + N_B$, following a Poisson distribution with mean $\mu = N_B$. A signal with more than 5σ statistical significance could already be observed with a luminosity of 5 fb^{-1} for a Higgs-boson mass between 150 and 180 GeV. In the next section systematic uncertainties on the backgrounds will be added to these results.

Figure 10 shows the $p_t^{\ell\,min}$ and $p_t^{\ell\,max}$ distributions for the sum of all backgrounds and the signal for a 165 GeV Higgs boson. A cut on the higher part of the $p_t^{\ell\,max}$ spectrum provides an additional background reduction.

For Higgs-boson masses between 160 GeV and 170 GeV the signal-to-background ratio is higher than one. The most important background component is continuum WW production. The inclusion of WW produced through gluon fusion increases this background source of about 30%.

The $t\bar{t}$ production is the dominant contribution from top, while tWb represents less than 15% of the $t\bar{t}$ contribution. The $t\bar{t}$ background was generated using TopReX. Two differences were observed when comparing the selection efficiency of this sample with a sample generated with PYTHIA. The efficiency of the $\phi_{\ell\ell}$ cut is about 0.14 for the PYTHIA sample whereas it is 0.18 for the TopReX sample, without applying the other kinematic cuts. This is due to the fact that TopReX includes spin correlations in the top production, leading to a slightly different shape in the $\phi_{\ell\ell}$ distribution. Figure 13 shows the $\phi_{\ell\ell}$ distribution for events with two good reconstructed leptons predicted by TopReX (solid line) and PYTHIA (dotted line).

[8] For a specific study of a Higgs with a lower or higher mass in this channel a better efficiency could be obtained by defining mass dependent cuts. This will be done in an upcoming CMS study.

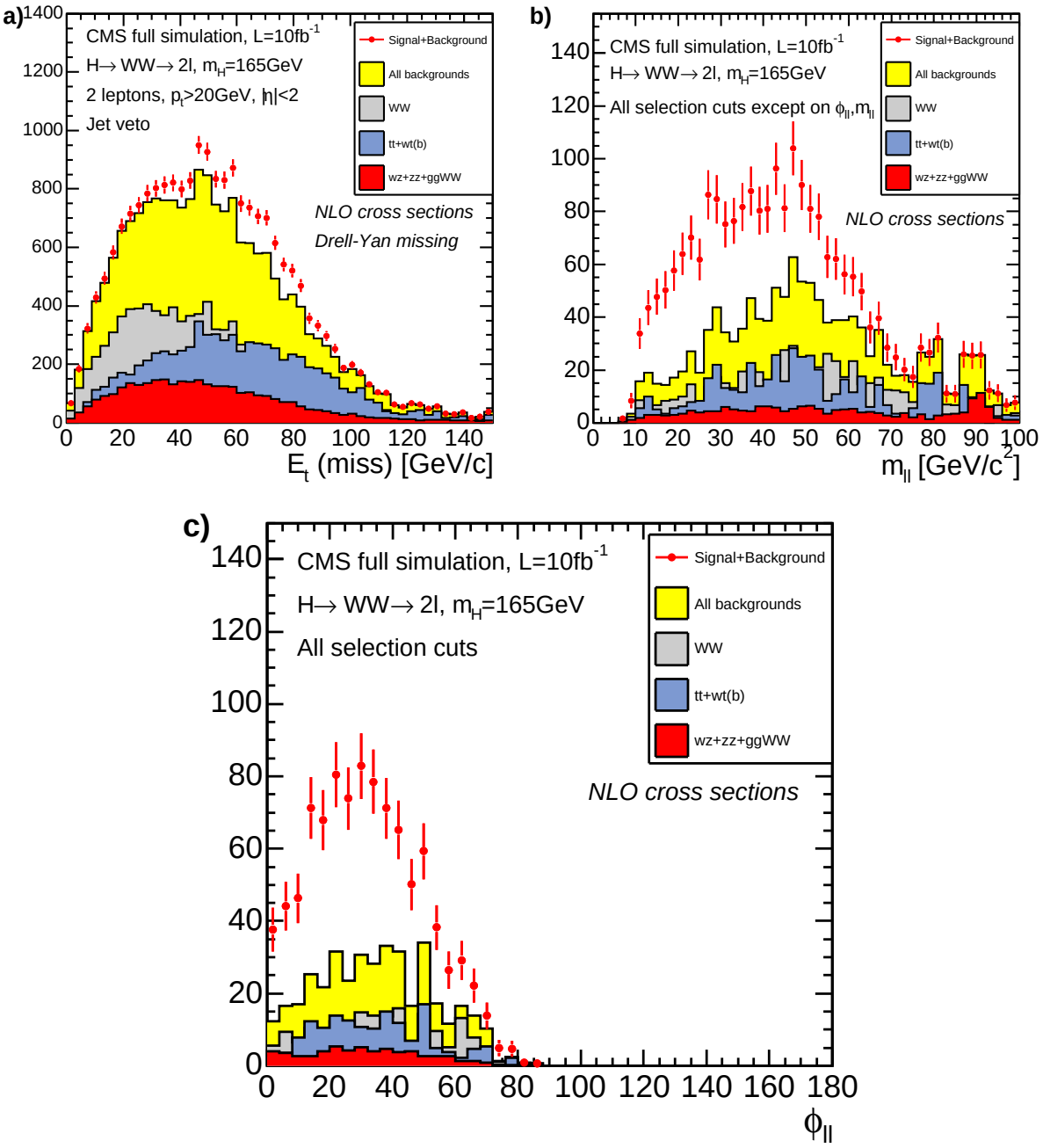

Figure 9: Distributions of selection variables for signal and the different backgrounds and an integrated luminosity of 10 fb^{-1}. The statistical uncertainties of the simulated data sample is shown. a) The missing energy distribution after requiring two good leptons and applying the jet veto (Drell-Yan is not shown on the plot but is expected to have a sharp peak around 15 GeV). b) The invariant mass of the two leptons after all selection cuts are applied except the ones on $m_{\ell\ell}$ and $\phi_{\ell\ell}$. c) The angle between the leptons in the transverse plane after all signal cuts excluding the one on $\phi_{\ell\ell}$.

The efficiency to keep background events after a jet veto is applied is also about 20% higher in the TopReX sample when no other kinematic cuts are applied. This might be due to the fact that TopReX allows no hard gluon emission from the top whereas PYTHIA does. When data will be available it will be possible to discriminate between these two predictions[9)].

The background contribution from WZ and ZZ is expected to be small, respectively 1.8% and 1.2% of the total background. The Drell-Yan background was not considered in this analysis. It was however checked using a

[9)] Issues related to top background simulation and systematics are discussed in detail in [11].

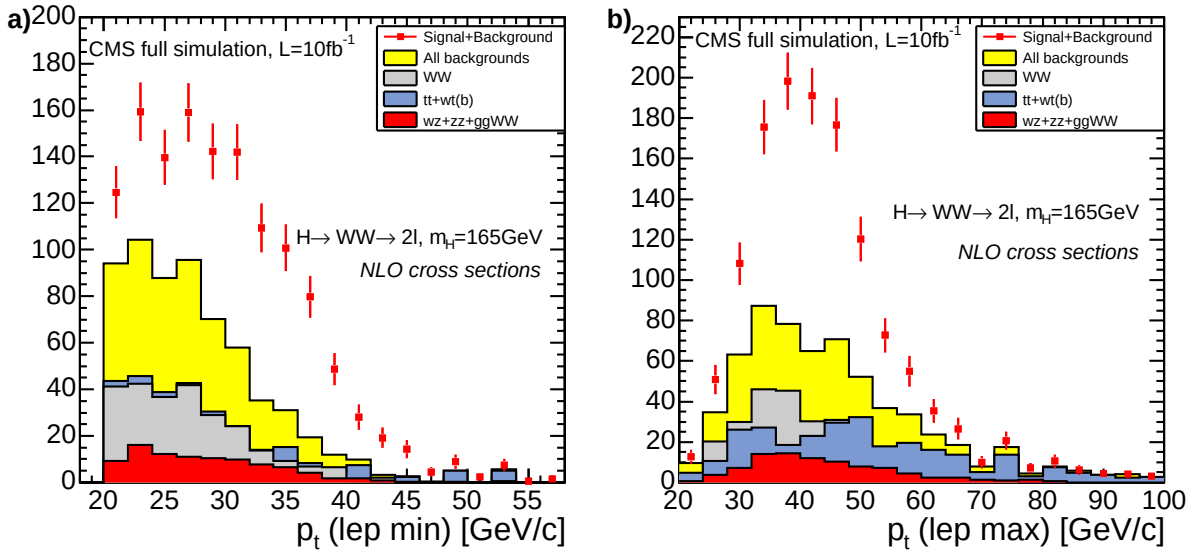

Figure 10: Distributions for a 165 GeV Higgs boson and the sum of all backgrounds after all other selection cuts are applied for the a) minimal and b) maximal lepton transverse-momentum. The statistical uncertainty of the simulated sample is shown.

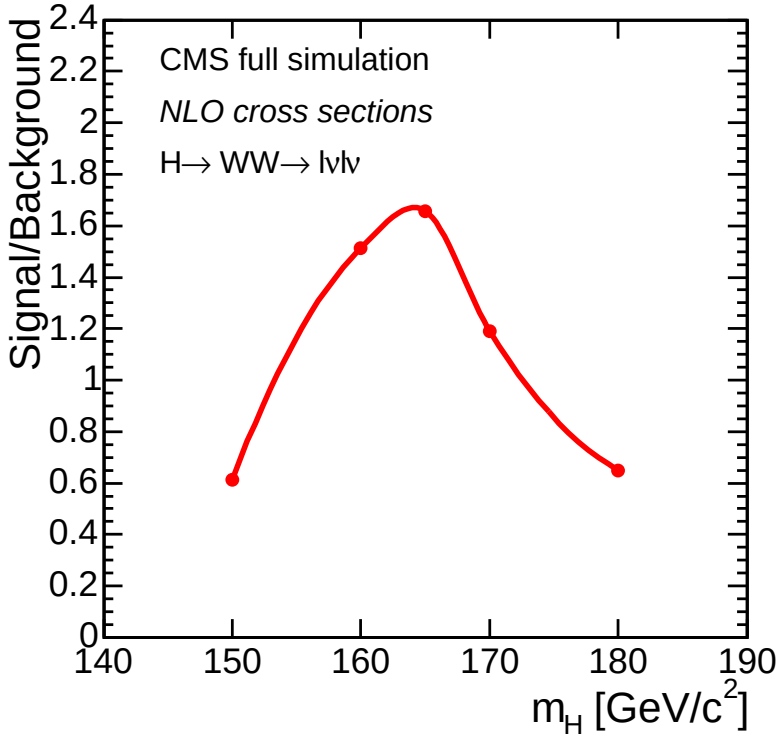

Figure 11: Signal-to-background ratio as a function of different Higgs-boson masses for the H → WW channel. No systematic uncertainties are included.

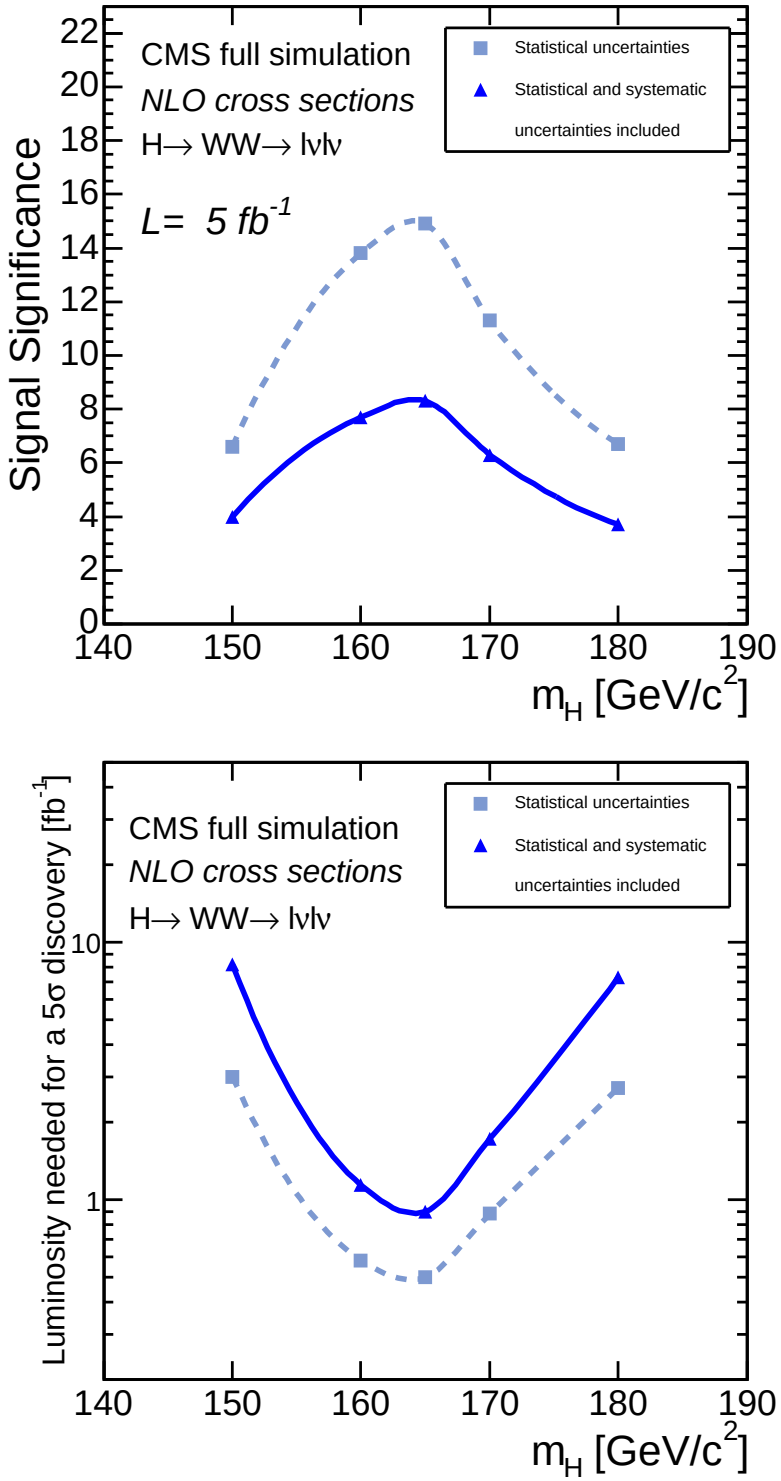

Figure 12: a) Signal significance for an integrated luminosity of 5 fb^{-1} and b) the integrated luminosity needed for a 5σ discovery as a function of different Higgs-boson masses for the H $\rightarrow$ WW channel. The dashed curve (squares) is with statistical errors only while the solid curve (triangles) also contains systematic uncertainties from background control and limited Monte Carlo statistics.

Table 8: The signal-to-background ratio for the different Higgs-boson masses together with the integrated luminosity needed for a 5σ discovery, with and without the inclusion of background uncertainties. For Higgs masses of 120-140 GeV and 190-200 GeV, the background uncertainties prevent a high significance observation.

m_H [GeV]	S/B	Significance for 5 fb^{-1}		$\mathcal{L}_{disc}$ [fb^{-1}]		
		no bkg syst	with bkg syst and MC stat	no bkg syst	with bkg syst	with bkg syst and MC stat
120	0.03	0.3	0.2	1100	-	-
130	0.12	1.3	0.7	72	-	-
140	0.30	3.3	1.8	12	-	-
150	0.61	6.6	4.0	3.0	7.1	8.2
160	1.51	14	7.7	0.58	1.0	1.1
165	1.66	15	8.3	0.50	0.81	0.90
170	1.19	11	6.3	0.88	1.5	1.7
180	0.65	6.7	3.7	2.7	5.7	7.3
190	0.33	3.6	2.0	10	-	-
200	0.22	2.2	1.2	27	-	-

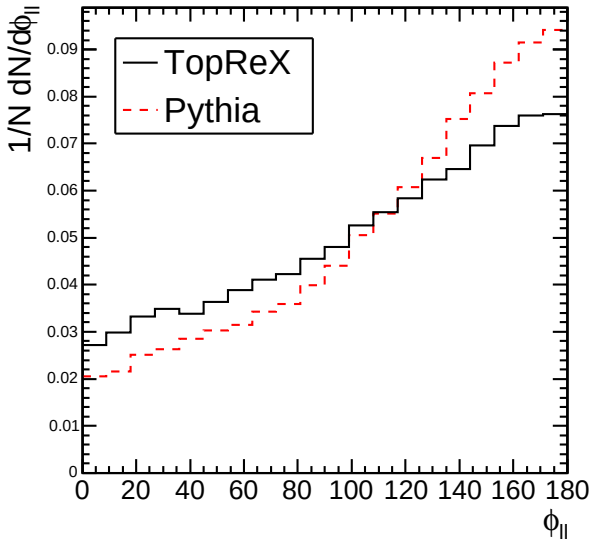

Figure 13: $\phi_{\ell\ell}$ distribution for events with two good reconstructed leptons predicted by TopReX (solid line) and PYTHIA (dashed line).

2.5 fb^{-1} sample of $pp \to \gamma, Z \to \mu\mu X$ (where the tau decays into muons were also simulated) that this background should represent less than 2% of the total background.

Table 9 compares the selection cut efficiencies for H $\to$ WW decays into two electrons, two muons and one electron and one muon. The W decays into τ were not taken into account here [10]. The trigger efficiency for the two-muon final state, 83%, is higher than for the two electron final state, 73%. Globally, the electron selection efficiency is lower due to the tracker material. The efficiency of the E_t^{miss} cut is also higher for the two muon final state, 74%, than for the two electron final state, 69%. This is probably due to the increased activity in the calorimeters when there are two electrons in the final state. The efficiencies of all other cuts are similar. These differences in the selection efficiencies between electron and muon final states are also observed for the different background samples.

[10] For a 165 GeV Higgs the WW decays including τ represent only 4% of the total signal.

Table 9: The expected number of events for an integrated luminosity of 1 fb^{-1} for a 165 GeV Higgs boson for the two-electron, two-muon and electron-muon final states. The relative efficiency with respect to the previous cut is given in parentheses. The W decay into τ are not taken into account. The last line shows the total selection efficiency together with the uncertainty from the limited Monte Carlo statistics.

$m_H = 165$ GeV	$WW \to ee$	$WW \to \mu\mu$	$WW \to e\mu$
$\sigma \times BR(e, \mu)$ [fb]	262	262	524
L1+HLT	190 (73%)	217 (83%)	394 (75%)
2 lep, $\lvert\eta\rvert < 2$, $p_t > 20$GeV $\sigma_{IP} > 3$, $\lvert\Delta z_{lep}\rvert < 0.2$ cm	77 (41%)	106 (49%)	176 (45%)
$E_t^{miss} > 50$ GeV	53 (68%)	79 (75%)	124 (71%)
$\phi_{\ell\ell} < 45$	30 (57%)	46 (58%)	71 (57%)
12 GeV $< m_{\ell\ell} <$ 40 GeV	22 (74%)	35 (76%)	53 (75%)
Jet veto	12 (52%)	19 (54%)	28 (53%)
30 GeV$< p_t^{\ell\,max} <$55 GeV	10 (87%)	16 (85%)	24 (86%)
$p_t^{\ell\,min} >$25 GeV	9.0 (90%)	14 (85%)	21 (87%)
ε_{tot}	$(3.4 \pm 0.2)\%$	$(5.3 \pm 0.3)\%$	$(4.0 \pm 0.2)\%$

5 Background Normalization and Systematics

At the LHC, it is desirable for the background to be determined from data whenever possible. This is relevant for the present study, which is a 'counting experiment'. In the case where backgrounds can be estimated using a normalization region in the data, the expected number of events for a background in the signal region, $N_{bkg}^{\text{signal region}}$, can be calculated using the following formula:

$$N_{bkg}^{\text{signal region}} = \frac{\varepsilon_{bkg}^{\text{signal region}}}{\varepsilon_{bkg}^{\text{normalization region}}} N_{bkg}^{\text{normalization region}} \tag{2}$$

where $N_{bkg}^{\text{normalization region}}$ is the number of background events in the normalization region, $\varepsilon_{bkg}^{\text{signal region}}$ and $\varepsilon_{bkg}^{\text{normalization region}}$ the efficiencies to select the background in the signal, respectively in the normalization region.

If similar cuts are used to define the signal and the normalization regions, most systematic errors will cancel in the efficiency ratio. Moreover the efficiency ratio is better controlled than the predictions for the single efficiencies.

Such a procedure can be used to determine the $t\bar{t}$, WW and WZ background. The other background components, ggWW and tWb, represent a small fraction of the total background. Currently no method has been proposed which allow to isolate them and their systematic uncertainties is determined using the Monte Carlo calculations.

Table 10: The different systematic uncertainties expected for the reconstructed objects for an integrated luminosity of 5 fb^{-1} [10].

	Systematic error at low luminosity
Lepton identification	3%
b-tagging	9%
Calorimeter energy scale	2%
Jet energy scale	7.5%

The values assumed for the systematic errors from the reconstruction are listed in Table 10.

5.1 $t\bar{t}$ background normalization

Two procedures are proposed to normalize the $t\bar{t}$ background and are explained in detail in reference [11]. The first one is based on a double b-tagging and the other one requires two hard E_t jets in the final state.

A first normalization region is defined by replacing the jet veto in the selection cuts by the requirement of two b-tagged jets in the final state. The other selection cuts are kept unchanged. For the b-tagging, one requires first two jets with $E_t > 20$ GeV and $|\eta| < 2.5$. A jet is then b-tagged if it has at least two tracks with an impact parameter significance higher than 2. The contribution from other backgrounds after the double jet veto is applied is expected to be less than 1% of the $t\bar{t}$ contribution.

A first source of systematics on this background normalization is the theoretical prediction of the ratio between the

numbers of events in the signal and in the normalization region. By varying the factorization and normalization scale, this error is expected to be around 5% [12]. The effect of introducing higher order corrections is expected to be small, since the signal region is dominated by LO processes after the jet veto is applied.

The jet energy scale is another source of uncertainty. It is expected to be around 7.5% with an integrated luminosity of 5 fb^{-1}. The effect of the jet energy scale error on the $\mathrm{t\bar{t}}$ background normalization can be estimated by recording how much the ratio $\varepsilon_{\mathrm{bkg}}^{\mathrm{sig\,reg}}/\varepsilon_{\mathrm{bkg}}^{\mathrm{norm\,reg}}$ varies when the jet energy scale is varied [11]. This variation is about 12% for a jet energy scale error of 7.5%. An error of about 4% is expected on the use of the alpha parameter in the jet reconstruction. Finally the b-tagging uncertainty is expected to be around 9% for an integrated luminosity of 5 fb^{-1}. The statistical uncertainties from the number of events in the normalization region are negligible here. Summing these uncertainties in quadrature, a global uncertainty of 16% is expected for an integrated luminosity of 5 fb^{-1}.

This b-tagging method is very promising but might be hard to apply on early data as the systematics of b-tagging might need understanding. A second possibility would be to replace the b-tagging by simply requiring two additional hard jets with respectively $\mathrm{E_t^{jet\,1}} > 50$ GeV and $\mathrm{E_t^{jet\,2}} > 35$ GeV. In this case, in order to avoid a contamination from Drell-Yan background, only $\mathrm{e}\mu$ final states are considered. The sources of systematics are 5% for the theoretical estimate, 15% for the jet energy scale and 4% for the jet reconstruction, for an overall uncertainty of 16%.

In both procedures, systematic uncertainties are larger than statistical uncertainties. It must be noted that this list of systematics might not be exhaustive once additional experimental and theoretical information will be available. With increasing luminosity, some improvements can be expected.

5.2 WW background normalization

A normalization region for WW can be defined by requiring $\phi_{\ell\ell} < 140$ and $\mathrm{m}_{\ell\ell} > 60$ GeV, keeping all other signal selection cuts unchanged. This mass cut eliminates essentially all events with a small $\phi_{\ell\ell}$. In this case and for an integrated luminosity of 5 fb^{-1}, the error on the theoretical prediction of the ratio between the number of WW events in the signal and in the normalization region is expected to be small compared to the other sources of uncertainty [13]. Only the $\mathrm{e}\mu$ final state is considered in order to reduce the contribution of Drell-Yan and WZ.

Figure 14 shows the $\phi_{\ell\ell}$ distributions for the different processes in this normalization region. For an integrated luminosity of 5 fb^{-1}, about 124 WW events are expected in this signal-depleted region, 88 from $\mathrm{t\bar{t}}$, and 30 events from the other backgrounds (12 from tWb, 12 from ggWW and 6 from WZ). An additional 28 signal events for a Higgs-boson mass of 165 GeV are expected, compared to 230 events in the signal region.

Systematic uncertainties of 16%, 20%, 22% and 30% can be expected on the $\mathrm{t\bar{t}}$, WZ, tWb and ggWW backgrounds respectively, as discussed in the previous and following sections. The systematic uncertainty on WW events is given by adding the statistical and systematic error in quadrature:

$$\sqrt{242 + (88 \cdot 0.16)^2 + (12 \cdot 0.2)^2 + (12 \cdot 0.3)^2 + (6 \cdot 0.2)^2} = 21.5$$

This represents a relative systematic error of $21.5/124 = 17\%$. With data, the WW background should be normalized assuming that no signal is present. Therefore, in presence of a signal, the WW background will be overestimated in a first step by about 10%. This estimation can be then refined in an iterative procedure. The statistical uncertainty is the dominant uncertainty on the WW background. With 60 fb^{-1}, this error should be reduced by a factor of 2.

In a further study, the uncertainty on WW could be reduced by combining more normalization regions. Moreover with a suitable Drell-Yan simulation, the inclusion of ee and $\mu\mu$ final states in the normalization region could increase the statistics, reducing the statistical uncertainty.

5.3 WZ background normalization

The WZ background can be normalized by keeping the same selection cuts as in the signal region but requiring an additional lepton in the final state. To gain statistics, the cuts on $\phi_{\ell\ell}$ and $\mathrm{m}_{\ell\ell}$ are removed. For an integrated luminosity of 5 fb^{-1}, about 36 WZ events and 14 $\mathrm{t\bar{t}}$ events are expected. Assuming a 16% accuracy on the $\mathrm{t\bar{t}}$

[11] This variation must be done simultaneously since the jet veto in the signal region and the request for two hard jets in the normalization region are not independent.

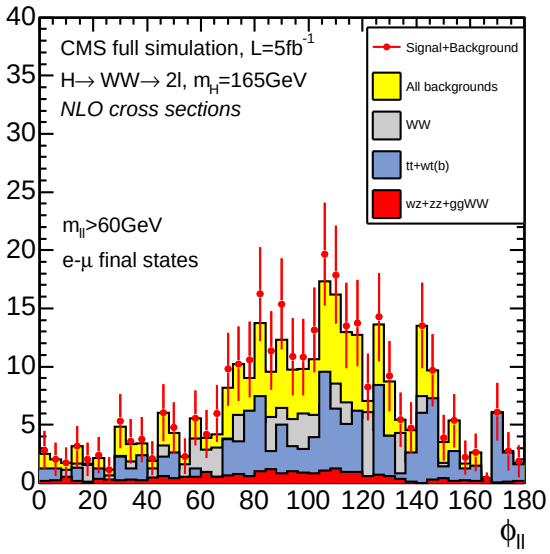

Figure 14: Distribution of the angle between the leptons in the transverse plane for the signal and the different backgrounds, for an integrated luminosity of 10 fb^{-1}. The WW normalization region is considered, with all signal cuts applied but $m_{\ell\ell} > 60$ GeV. Only electron-muon states are kept.

background and an additional 3% for the selection of the additional lepton, an accuracy of about 20% is expected on WZ with 5 fb^{-1}.

5.4 ggWW and tWb normalization

It is difficult to define a normalization region for the ggWW and tWb backgrounds. The Monte Carlo models can be used to predict them, since they represent only a small fraction of the background events. The systematic uncertainty is then given by the following formula:

$$\Delta N_{bkg} = \Delta_{stat} \oplus \Delta_{2\,lep} \oplus \Delta_{jet\ veto} \oplus \Delta_{missing\ energy} \oplus \Delta_{theory} \quad (3)$$

The error on the jet veto and the missing energy was determined by the variation in the global selection efficiency after varying respectively the jet energy by $\pm 2\%$ and the missing energy value by $\pm 2\%$. The theoretical uncertainty on ggWW is about 30% whereas for tWb it is about 20% [15]. Table 11 summarizes the different sources of systematic errors on these two backgrounds. The theoretical uncertainty are dominant.

Table 11: Systematic sources of uncertainty on the single resonant top production and continuum WW production via gluon fusion.

Systematic source	tWb	ggWW
Lepton identification	4.2%	4.2%
Missing energy	<1%	3%
Calorimeter energy scale	9%	1.5%
Theoretical error	20%	30%
Total	22%	30%

The ZZ background was not considered in the systematics study since it is expected to make a contribution of only 1.2% to the background in the signal region.

5.5 Effect of systematics on the signal significance

The signal significance is degraded by the introduction of systematics uncertainties on the background. This background uncertainty, ΔN_B, is taken into account by applying a Gaussian smearing of $\sigma = \Delta N_B$ on the number of expected background events [16]. For a large number of events, the significance, taking into account the background uncertainties, can be expressed with the following formula:

$$\text{Significance} = \frac{\mathrm{N_S}}{\sqrt{\mathrm{N_B} + \Delta \mathrm{N_B^2}}} \tag{4}$$

In this analysis, two sources of background uncertainty are considered: background normalization and section and limited Monte Carlo statistics. Taking into account the sum of the different backgrounds, an overall uncertainty of 10% is found on the total background if only the background systematics are considered. Adding the contribution from limited Monte Carlo statistics, this uncertainty increases to 13%. These results are calculated for an integrated luminosity of 5 fb^{-1}. For integrated luminosities of 1,2 and 10 fb^{-1}, the total systematic uncertainties scales to 19%, 16% and 11%, respectively. Figure 12 and Table 8 show the signal significance after the systematic uncertainties are taken into account. For a Higgs-boson mass of 165 GeV, the inclusion of background systematics increases the luminosity needed for a 5σ discovery by a factor 1.8, going from 0.5 fb to 0.9 fb. Due to the high signal-to-background ratio of 1.7, the signal is less sensitive to background fluctuations, leading to this restricted change in the required luminosity for a discovery.

For Higgs-boson masses higher than 180 GeV and lower than 150 GeV, the inclusion of background systematics prevents a 5σ discovery. The reason is that the signal to background ratio is lower than 0.5 in these regions. In this study we concentrated on the mass region around $\mathrm{m_H} = 165$ GeV. The selection cuts were optimized for this region. In principle the sensitivity of this channel could be increased by specifically tuning the cuts on the $\mathrm{p_t}$ of the leptons [1]. Moreover one might also expect that, with more luminosity, the background systematics can be further reduced.

6 Conclusion

Using a full CMS detector simulation and including background uncertainties, we showed that the Standard Model Higgs boson could be discovered in the $\mathrm{H} \rightarrow \mathrm{WW} \rightarrow \ell\nu\ell\nu$ channel with less than 1 fb^{-1} if its mass is around 165 GeV. If it has a mass between 150 and 180 GeV, a 5σ signal could be seen with a luminosity of about 10 fb^{-1}.

Acknowledgments
We would like to thank Fabio Maltoni, John Campbell and Nikolas Kauer for the useful discussions on how to generate the different backgrounds. We are thankful to Marco Zanetti for the nice collaboration on $t\bar{t}$ simulation issues and background normalization and A. Nikitenko for his help on the topic. Our thanks go also to the other people working on this channel, V. Drollinger, E. Delmeire, C. Rovelli and E. Torassa for many discussions on the subject. Finally we would like to thank Savaltore Mele for his careful re-reading and comments.

References

[1] M. Dittmar and H. K. Dreiner, "How to find a Higgs boson with a mass between 155-GeV to 180-GeV at the LHC", Phys. Rev. D **55** (1997) 167 [arXiv:hep-ph/9608317]

CMS NOTE-1997/083 M. Dittmar and H. K. Dreiner, *LHC Higgs Search with l+nul- nubar Final States*

[2] Cross sections calculated by M. Spira for the CMS Physics Technical Design Report

[3] S. Frixione and B. R. Webber, "Matching NLO QCD computations and parton shower simulations", JHEP **0206** (2002) 029 [arXiv:hep-ph/0204244]
S. Frixione, P. Nason and B. R. Webber, "Matching NLO QCD and parton showers in heavy flavour production", JHEP **0308** (2003) 007 [arXiv:hep-ph/0305252].

[4] G. Davatz, G. Dissertori, M. Dittmar, M. Grazzini and F. Pauss, "Effective K-factors for $\mathrm{gg} \rightarrow \mathrm{H} \rightarrow \mathrm{WW} \rightarrow \ell\nu\ell\nu$ at the LHC", JHEP **0405** (2004) 009 [arXiv:hep-ph/0402218]

[5] T. Binoth, M. Ciccolini, N. Kauer and M. Kramer, JHEP **0503** (2005) 065, [arXiv:hep-ph/0503094]

[6] S.R. Slabospitsky, L. Sonnenschein, Comput. Phys. Commun. **148** (2002) 87, [arXiv:hep-ph/0201292]

[7] J. Campbell and F. Tramontano, "Next-to-leading order corrections to W t production and decay", [arXiv:hep-ph/0506289] and "Les Houches 'Physics at TeV Colliders 2005' Higgs Working Group: Summary report," to be published.

[8] The WW, WZ, ZZ, tWb cross sections are calculated by J. Campbell using MCFM. The ggWW cross section is from reference [5]. The $t\bar{t}$ cross section is from reference [9].

[9] R. Bonciani, S. Catani, M. L. Mangano and P. Nason, "NLL resummation of the heavy-quark hadroproduction cross-section," Nucl. Phys. B **529** (1998) 424 [arXiv:hep-ph/9801375].

[10] Following the prescriptions of the CMS PRS group.

[11] **CMS NOTE-2006/048** G. Davatz, A.-S. Giolo-Nicollerat, M. Zanetti, *Systematic uncertainties of the top background in the H→WW channel*

[12] N. Kauer, "Top background extrapolation for H → W W searches at the LHC," Phys. Rev. D **70** (2004) 014020 [arXiv:hep-ph/0404045].

[13] **CMS NOTE 2005/024** V. Drollinger et al., *Modeling the production of W pairs at the LHC*

[14] Les Houches 2005 physics at hadron colliders proceedings, to be published

[15] N. Kauer and J. Campbell, private communication.

[16] The significance is calculated using the "scp" program: Bityukov et al., Program for evalutation of the significance, confidence intervals and limits by direct calculation of prbabilities, PHYSTAT'05 proceedings, http://www.physics.ox.ac.uk/phystat05/ proceedings/files/bityukov-talk2_final.pdf